NEOPLASIA
www.neoplasia.com

Volume 18 Number 12 December 2016 pp. 795–805 795

Patient-Specific Screening Using High-Grade Glioma Explants to Determine Potential Radiosensitization by a TGF-β Small Molecule Inhibitor[1,2]

N. Sumru Bayin[*,†,3,4], Lin Ma[‡,3], Cheddhi Thomas[§], Rabaa Baitalmal[§], Akhila Sure[*], Kush Fansiwala[*], Mark Bustoros[*], John G. Golfinos[*,¶,#], Donato Pacione[*], Matija Snuderl[§,¶,#], David Zagzag[§,¶,#], Mary Helen Barcellos-Hoff[‡] and Dimitris Placantonakis[*,†,¶,#]

*Department of Neurosurgery, NYU School of Medicine; [†]Kimmel Center for Stem Cell Biology, NYU School of Medicine; [‡]Department of Radiation Oncology, University of California, San Francisco; [§]Department of Pathology, NYU School of Medicine; [¶]Perlmutter Cancer Center, NYU School of Medicine; [#]Brain Tumor Center, NYU School of Medicine

Abstract

High-grade glioma (HGG), a deadly primary brain malignancy, manifests radioresistance mediated by cell-intrinsic and microenvironmental mechanisms. High levels of the cytokine transforming growth factor-β (TGF-β) in HGG promote radioresistance by enforcing an effective DNA damage response and supporting glioma stem cell self-renewal. Our analysis of HGG TCGA data and immunohistochemical staining of phosphorylated Smad2, which is the main transducer of canonical TGF-β signaling, indicated variable levels of TGF-β pathway activation across HGG tumors. These data suggest that evaluating the putative benefit of inhibiting TGF-β during radiotherapy requires personalized screening. Thus, we used explant cultures of seven HGG specimens as a rapid, patient-specific *ex vivo* platform to test the hypothesis that LY364947, a small molecule inhibitor of the TGF-β type I receptor, acts as a radiosensitizer in HGG. Immunofluorescence detection and image analysis of γ-H2AX foci, a marker of cellular recognition of radiation-induced DNA damage, and Sox2, a stem cell marker that increases post-radiation, indicated that LY364947 blocked these radiation responses in five of seven specimens. Collectively, our findings suggest that TGF-β signaling increases radioresistance in most, but not all, HGGs. We propose that short-term culture of HGG explants provides a flexible and rapid platform for screening context-dependent efficacy of radiosensitizing agents in patient-specific fashion. This time- and cost-effective approach could be used to personalize treatment plans in HGG patients.

Neoplasia (2016) 18, 795–805

Introduction

High-grade gliomas (HGGs), including glioblastomas (GBMs) and anaplastic gliomas, are the most common primary brain malignancy with 10,000 to 15,000 new cases in the United States annually (http://www.cbtrus.org). Despite aggressive surgical removal and concomitant chemoradiotherapy, median survival remains at 14 to 16 months [1,2]. Recent sequencing efforts have classified GBM tumors into molecular subtypes identified by distinct genetic alterations [3,4]. However, current radiation schedules and chemotherapy protocols fall in the "one size fits all" category [1] and fail to take into account this intertumoral heterogeneity. In light of the mismatch between uniform treatments and this heterogeneous malignancy, the concept of personalized treatment plans has been gaining traction in recent years.

Address all correspondence to: Dimitris G. Placantonakis, MD, PhD, Department of Neurosurgery, NYU School of Medicine, 530 First Avenue, Skirball 8R, New York, NY 10016, USA, or Mary Helen Barcellos-Hoff, PhD, Department of Radiation Oncology, University of California, San Francisco, 2340 Sutter Street, San Francisco, CA 94115, USA.
E-mails: Dimitris.Placantonakis@nyumc.org, mary.barcellos-hoff@ucsf.edu

[1] Conflicts of interest: none.

[2] This research was supported by the National Institutes of Health (1R21NS088775-01 to D.G.P. and M.H.B.-H). N. S. B. received support from NYSTEM Institutional training grant #CO26880.

[3] Equal contribution.

[4] Current address: Developmental Biology Program, Sloan Kettering Institute.

Received 14 July 2016; Revised 26 August 2016; Accepted 29 August 2016

1476-5586
http://dx.doi.org/10.1016/j.neo.2016.08.008

HGG shows profound radioresistance so that treatment requires high doses and large fields of ionizing radiation (IR). Even then, and despite concurrent and adjuvant treatment with the alkylating agent temozolamide [1], HGG inevitably recurs and progresses. Stem-like tumor cells, namely glioma stem cells (GSCs), have been linked to tumor recurrence [5–7]. These cells, besides having the ability to self-renew and efficiently initiate tumors in animal models, are equipped with cell-intrinsic mechanisms that confer robust radioresistance due to enhanced DNA damage response (DDR) [7]. Signaling pathways associated with self-renewal are also important for GSC survival after radiation [8–14]. Moreover, the brain and tumor microenvironment (TME) are critical for the response to radiotherapy, as exemplified by human GSCs identified by cell surface expression of CD133 that display radiosensitivity *in vitro* but become profoundly radioresistant when implanted into the mouse brain [15]. Given the importance of both cell-intrinsic and -extrinsic mechanisms that confer resistance to radiotherapy, preclinical studies of radiosensitizing agents require a contextual testing platform that takes into account GSC biology, the TME, and the intertumoral heterogeneity of HGGs.

One of the key components of the HGG TME is the pleotropic cytokine transforming growth factor-β (TGF-β), whose downstream signaling regulates several processes related to tumor progression, including matrix deposition, angiogenesis, and brain invasion [16–21]. The TGF-β type II receptor is responsible for binding TGFβ1, TGFβ2, or TGFβ3 ligands and then recruits type I receptors (TGFβRIs) to form a heterotetrameric complex that initiates downstream signaling *via* serine phosphorylation of Smad2 [21,22]. Our previous studies implicate TGF-β in GBM radioresistance and GSC self-renewal [8,10,23]. We showed that pharmacologic TGF-β inhibition in murine and human GBM cell lines prior to radiation decreases DDR, increases tumor cell kill, and abolishes GSC resistance, which together improve response to fractionated radiation therapy in a preclinical model [8]. Huber and colleagues also reported that a small molecule inhibitor of the TGFβRI (ALK5) kinase activity is effective in combination with radiation and temozolamide [10,23]. Importantly, TGF-β inhibitors are currently in clinical trials to treat recurrent HGG, with favorable responses observed in some patients [16,24–27].

Given the molecular heterogeneity across HGG tumors and the possibility that distinct tumors may respond differentially to radiotherapy and TGF-β inhibition, we set out to develop an *ex vivo* platform to test radioresponse for individual patients. Because the effects of radiation on HGG tissue are mediated by both cell-intrinsic properties and the TME, we reasoned that personalized radiation biology could be improved by maintaining critical cancer cell-TME interactions in human specimens. Tabar and colleagues recently introduced HGG organotypic cultures that preserve tissue architecture and TME and have been used to study several aspects of tumor biology [28–30]. We hypothesized that such cultures of human HGG specimens could serve as an *ex vivo* system to study radioresponse in a personalized manner.

Here, we tested responses to IR and TGF-β inhibition by LY364947, an antagonist of TGFβRI kinase activity (RIKI), in human HGG explants. We show that recognition of radiation-induced DNA double-strand breaks (DSBs) marked by γ-H2AX and the post-radiation increase in the GSC self-renewal marker Sox2 [31] are blocked by RIKI in most, but not all, patient-derived explants. This study serves as proof-of-principle demonstration that TGF-β inhibition represents a robust approach to compromise DDR, and presumably increase tumor cell kill, in the majority of HGGs. Furthermore, as candidate responders were identified using screening *ex vivo* within a week of surgery, HGG patient stratification using explant cultures is a viable approach toward personalized precision medicine. We propose that the preservation of tumor cell-TME interactions in these explants renders them a highly adaptable *ex vivo* drug screening platform for testing agents that affect complex biological processes, such as radioresponse.

Materials and Methods

Analysis of TCGA Gene Expression Data

The UCSC Cancer Browser (https://genome-cancer.ucsc.edu) was used to analyze TCGA RNA-seq data of 172 GBM patients. The database was interrogated for expression levels of six transcripts (*TGFB1*, *TGFB2*, *TGFB3*, *TGFBR1*, *TGFBR2*, and *TNC*) and grouped according to the origin of the specimen (normal brain, newly diagnosed tumor, recurrent tumor). Data were exported to Prism for statistical analysis with analysis of variance (ANOVA) and *post hoc* Tukey test. Significance was set at $P < 0.05$. Data were plotted as box and whisker plots, showing the median, first and third quartiles (box), and min to max (whiskers).

Grading of GBM Specimens Based on p-Smad2 Immunoreactivity

We analyzed 14 formalin-fixed paraffin-embedded (FFPE) human HGG biospecimens from 12 patients (Supplemental Table 1) for phosphorylated Smad2 immunoreactivity (p-Smad2; cat. #3108, Cell Signaling Technology, Danvers, MA) using immunohistochemical techniques [32]. Antibody optimization was performed on 4-μm sections. We regarded cells clearly showing nuclear labeling as positive. Chromogenic immunohistochemistry was performed on a Ventana Medical Systems Discovery XT instrument with online deparaffinization using Ventana's reagents and detection kits (Ventana Medical Systems Tucson, AZ). p-Smad2 was antigen-retrieved in Ventana Cell Conditioner 1 (Tris-Borate-EDTA) for 20 minutes. Antibody against p-Smad2 was diluted 1:100 in Cell Signaling Antibody Diluent (cat. #8112, Cell Signaling Technologies) and incubated for 3 hours at room temperature. Primary antibody was detected with anti-rabbit secondary antibody conjugated to horseradish peroxidase for 8 minutes. The complex was visualized with 3,3′-diaminobenzidene and enhanced with copper sulfate. Slide were washed in distilled water, counterstained with hematoxylin, dehydrated, and mounted with permanent media. Negative controls were incubated with Dulbecco's phosphate-buffered saline (PBS) instead of primary antibody.

Staining intensity was graded by two observers according to the following criteria: no staining, grade –; <1% of tumor cells, grade +; 1% to 10% of tumor cells, grade ++; 10% to 50% of tumor cells, grade +++; and >50% of tumor cells, grade ++++. We have used this approach previously for grading immunohistochemical signal in surgical specimens [33].

Molecular Subtyping of Primary HGG Specimens

We followed a protocol approved by NYU Langone Medical Center's Institutional Review Board to procure fresh tumor tissue from patients undergoing surgery for resection of HGG (Institutional Review Board #12-01130). Diagnosis and grade of the specimens were confirmed by reviewing hematoxylin and eosin slides. Parental tumors were molecularly classified using genomic DNA extracted

from FFPE tissue and analyzed with Infinium 450K DNA methylation arrays (Supplemental Table 2 and Supplemental Figure 1), as previously described [34]. Briefly, the DNA was bisulfite-converted using the EZ-96 DNA Methylation Kit (Zymo Research). After the unmethylated cytosines were deaminated, the DNA then underwent restoration using the Illumina Infinium HD FFPE DNA Restore Kit, followed by whole-genome overnight amplification. The amplified DNA was then enzymatically fragmented using end-point fragmentation, isolated, precipitated in isopropanol, and resuspended in Illumina RA1 buffer. The resuspended DNA was then denatured at 95°C, and the resulting single-stranded DNA was dispensed directly onto the Illumina Human Methylation 450 BeadChip Array for hybridization overnight at 48°C. After hybridization, the BeadChips were washed with Illumina PB1 buffer to remove any unhybridized and nonspecifically hybridized DNA. Using Tecan Te-Flow, labeled nucleotides were dispensed over the BeadChips in flow-through chambers to extend primers hybridized to the DNA. The primers were then fluorescently stained, and the BeadChips were coated in Illumina XC4 buffer to protect the fluorescence before scanning. Once the BeadChips were scanned, raw data files containing the fluorescence intensity data for each probe were generated. Illumina Infinium HumanMethylation450 BeadChip arrays were analyzed using the R package RnBeads version 1.0.0 [35]. Briefly, probes overlapping single nucleotide polymorphisms ($n = 4713$) were removed. The remaining probes were background-corrected using the "noob" method of the methylumi package [36], and β values were normalized using the β-mixture quantile method [37].

DNA methylation profiling can reliably identify RTK1-type GBM [34], which corresponds to the proneural subtype described by Verhaak et al. [3]. However, DNA methylation cannot by itself reliably distinguish between mesenchymal and classical GBM [3,34]. For the sake of simplicity, we will use the term "non-RTK1 GBM" for such tumors (Supplemental Table 2).

HGG Explant Culture System

Our protocol was modified from the GBM organotypic culture method previously described [28]. Fresh specimens were transported to the laboratory in ice-cold Hank's buffered saline solution (Gibco) within 30 minutes after resection. Gelatinous tumor tissue was diced to roughly 0.5-mm^3 pieces using sterile surgical blades on a sterile 100-mm Petri dish on ice. Necrotic areas were discarded, as previously described [28]. Tissue pieces were transferred onto Laminin (20 μg/ml, cat. #L2020, Sigma)-coated Transwell inserts (cat. #3414, Corning) and placed in wells in which the lower compartment contained Neurobasal Media (cat. #21103049, Gibco) supplemented with N2 (cat. #A1370701, Gibco), B27 (cat. #12,587,010, Gibco), 20 ng/ml of epidermal growth factor (cat. #PHG0311, Life Technologies), and 20 ng/ml of fibroblast growth factor 2 (cat. #PHG0021, Life Technologies). Tissue pieces were wet with 10 μl of media on a daily basis to prevent them from drying out. The medium in the lower compartment was changed every other day. At least three pieces of tissue from each specimen were used for each treatment condition studied. Explant cultures were maintained in a 37°C incubator whose atmosphere contained 21% O_2 and 5% CO_2.

Irradiation and Sample Collection

HGG explants were irradiated with 2 Gy using 225-kV X-rays with an Xstrahl small animal radiation research platform (Surrey, UK). Samples were collected 30 or 60 minutes after irradiation. Cultured tissue was frozen in Optimal Cutting Temperature compound (Tissue-Tek) and cryosectioned at 5-μm thickness.

Activation and Inhibition of TGF-β Signaling

To assess the responsiveness of explants to TGF-β, cultures were treated with TGF-β (2 ng/ml; cat. #240-B-002, R&D Systems) given 30 minutes prior to collection. TGF-β signaling was blocked with the TGF-β receptor I inhibitor LY364947, referred to as RIKI (2 μM; Millipore, cat. #616,451), administered 24 hours prior to collection. TGF-β responsiveness and efficacy of inhibition with RIKI were assessed by p-Smad2 immunostaining, as described below.

Immunofluorescence Staining

Cryosections were fixed using 4% paraformaldehyde for 20 minutes at room temperature. Sections were blocked with 0.5% casein in PBS and incubated with the following antibodies: mouse anti–γ-H2AX at 1:200 (cat. #05-636, Millipore); rabbit anti-phosphoserine 465/467 Smad2 (p-Smad2) at 1:50 (clone138D4, cat. #3108, Cell Signaling); rabbit anti-CD45 (cat. #Ab10558, Abcam) at 1:200; and goat anti-Sox2 at 1:50 (cat. #AF2018, R&D Systems). Primary antibody incubations were carried out overnight at 4°C, followed by washes and 1-hour incubation with Alexa488- or Alexa594-labeled anti-mouse, anti-rabbit, or anti-goat secondary antibodies (Molecular Probes) at room temperature. Nuclei were stained with 4′,6-diamidino-2-phenylindole (DAPI). Sections were washed in PBS-Tween20 (0.1%) before mounting with Vectashield mounting medium (Vector Labs).

Image Acquisition and Quantification

Specimens were imaged using a 40× Zeiss Plan-Apochromat objective with 0.95 numerical aperture on a Zeiss Axiovert (Zeiss) epifluorescent microscope. All images were acquired with a CCD Hamamatsu Photonics (Herrsching am Ammersee, Germany) monochrome camera at 1392 × 1040 pixel size, 12 bits per pixel depth, and assembled as false-color images using the Metamorph imaging platform (Molecular Devices, Inc.).

For quantitation of cells immunoreactive for p-Smad2, three to five nonoverlapping images were obtained per section and analyzed using in-house algorithms in Fiji-Image J (NIH, Bethesda, MA). Nuclear masks based on DAPI served to determine the regions of interest (ROIs). The fraction of p-Smad2–positive pixels in each ROI was calculated. A threshold value that discriminates between positive and negative cells was determined using all ROIs. The nuclear immunofluorescence intensity of Sox2 was similarly quantified. γ-H2AX foci were enumerated using an algorithm similar to that previously described [38]. The mean number of γ-H2AX foci as a function of treatment was determined only from positive cells (i.e., nuclei with one or more foci). To quantitate nuclear size after irradiation, we used SigmaScan Pro 5 (Systat Software Inc.) to measure dimensions of 524 nuclei defined by ROIs.

Statistical Analysis

Prism (Graphpad) software was used for statistical analysis. Statistical comparisons were calculated using Student's two-tailed *t* test or one-way ANOVA with *post hoc* Tukey test for multiple comparisons. Correlations were evaluated with Spearman's rank correlation coefficient and linear regression analysis. Data are presented as mean ± standard error. The number of patient samples

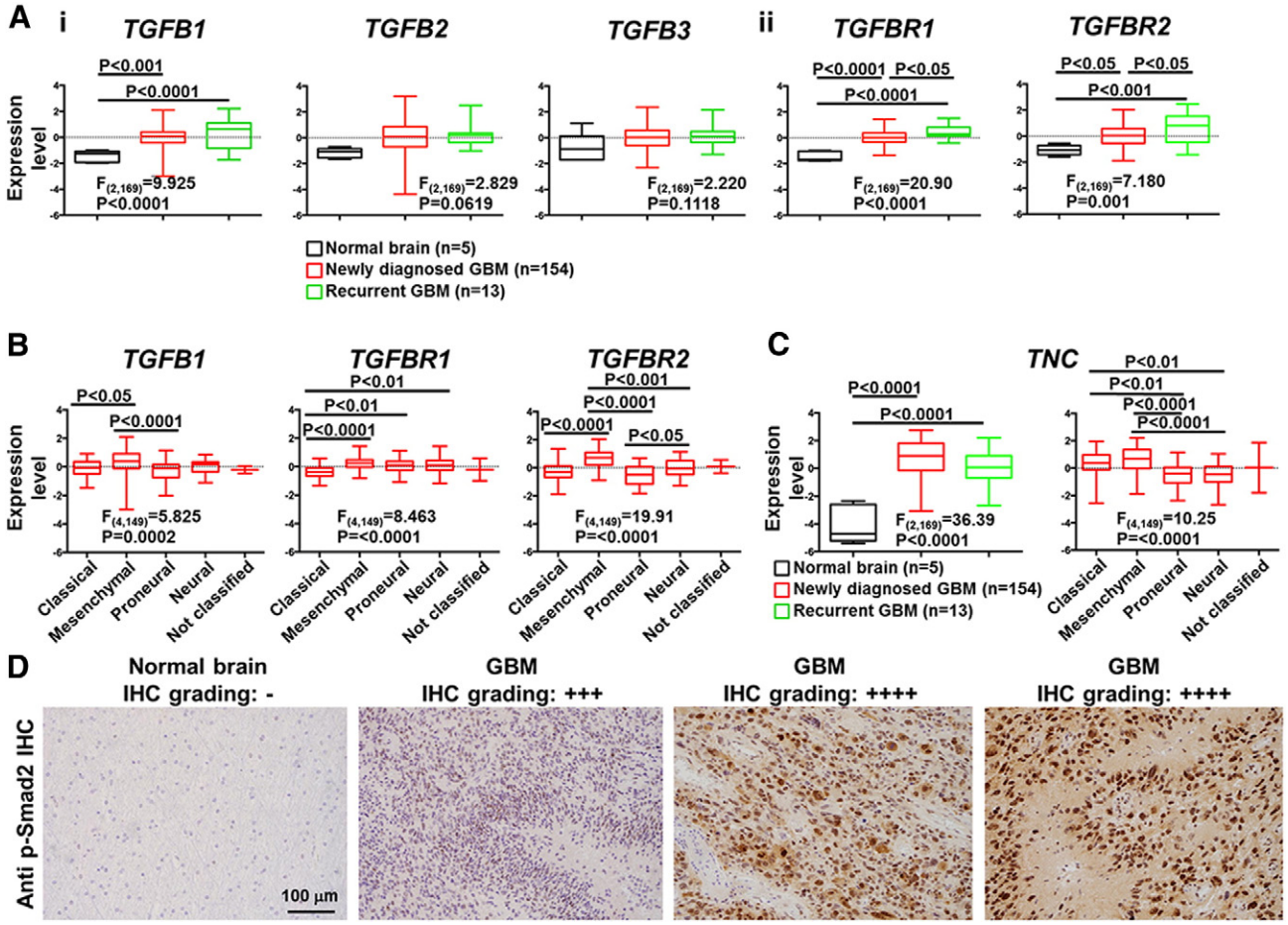

Figure 1. Heterogeneous activation of TGF-β signaling in HGGs. (A) Analysis of TCGA data on expression levels of five transcripts related to TGF-β signaling in GBM specimens (i: TGF-β ligands, ii: TGF-β receptors). For each transcript, expression levels across three different groups, normal brain (black), newly diagnosed GBM (red), and recurrent GBM (green), have been plotted as box-whisker plots. (B) Expression levels of transcripts *TGFB1*, *TGFBR1*, and *TGFBR2* across different molecular subgroups of GBM. (C) Analysis of *TNC* mRNA levels, a downstream target of TGF-β signaling, in normal brain (black), newly diagnosed GBM (red), and recurrent GBM (green). ANOVA statistics with *post hoc* comparisons were used in A to C. (D) Representative images of the grading system used to analyze p-Smad2 immunostaining in normal brain and HGG specimens.

analyzed (n) is designated in each analysis. Statistical significance was set at $P < 0.05$.

Results

Intertumoral Variability in TGF-β Signaling in TCGA Data and HGG Specimen Immunohistochemistry

The Cancer Genome Atlas (TCGA; http://cancergenome.nih.gov/) was interrogated for expression levels of mRNA transcripts encoding TGF-β isoforms (*TGFB1*, *TGFB2*, *TGFB3*; Figure 1*Ai*) and the TGF-β type I and II receptors (*TGFBR1 and TGFBR2*; Figure 1*Aii*) in newly diagnosed (n = 154) and recurrent (n = 13) GBM, the most common form of HGG, compared with normal brain (n = 5). The specimens from recurrent tumors are very likely to have been irradiated because the standard-of-care treatment for newly diagnosed HGG is surgery followed by concurrent chemoradiotherapy [1]. A robust and significant increase in expression of *TGFB1* and *TGFBR1* was evident between normal brain and GBM (Figure 1, *Ai* and *ii*). *TGFB2* trended toward significance (P = .06), but *TGFB3* did not. *TGFBR1* and *TGFBR2* were significantly increased in recurrent, very likely irradiated, tumors compared with newly diagnosed tumor (Figure 1*Aii*). These findings support the idea that TGF-β pathway is aberrantly activated in GBM and in response to therapy.

GBM is classified into four molecular subgroups by RNA sequencing and dominant driver mutations: classical, mesenchymal, proneural, and neural [3]. *TGFB1*, *TGFBR1*, and *TGFBR2* mRNA transcripts were differentially expressed among GBM subgroups (Figure 1*B*). Consistent with this, *tenascin C (TNC)* mRNA [39–41], a TGF-β target, was also significantly higher in both newly diagnosed and recurrent GBM compared with normal brain (Figure 1*C*). Within GBM, *TNC* expression was also differentially expressed across molecular subtypes, similar to *TGFB1*, *TGFBR1*, and *TGFBR2* (Figure 1*C*). The differences in expression of TGF-β pathway components among GBM molecular subtypes suggest that its activity may vary in tumors.

The key event in the canonical signal transduction pathway downstream of TGF-β receptor activation involves phosphorylation of Smad2 [20,22]. Upon ligand binding, TGF-β type II receptor dimers recruit, phosphorylate, and activate TGF-β type I receptor dimers. Active type I receptor, in turn, phosphorylates Smad2

(p-Smad2), which is the primary transducer of TGF-β signaling. Activation of the pathway causes a transient accumulation of p-Smad2 in the nucleus. To confirm whether the TGF-β pathway is activated in HGGs, as suggested by our TCGA analysis, we stained 14 FFPE HGG specimens from 12 patients for phosphorylated Smad2 (p-Smad2) (Figure 1*D* and Supplemental Table 1). We used a grading system based on the fraction of tumor cells that stain positive (see Methods). Normal brain was graded as negative for p-Smad2 immunostaining (–) (Figure 1*D*). In contrast, all HGG specimens stained positive with p-Smad2 at varying levels, analyzed by two independent observers (R.B. and D.Z.) (Figure 1*D*). The extent of the staining was variable and even included small sections of tumors with little to no staining in three specimens. However, the sample size was too small to identify specific correlations between the staining intensity and pathobiology (Supplemental Table 1). Collectively, these studies provide robust confirmation of the idea that TGF-β signaling is active in HGG, consistent with prior observations [20], but also indicate that the extent of activation of the pathway may vary among tumors.

Ex vivo Analysis of HGG Response to Radiation

To test the hypothesis that TGF-β signaling may regulate the response to radiation in human HGG tissue, we established explant cultures from seven surgical HGG specimens, all procured at NYU School of Medicine. The success rate of establishing viable explant cultures was 100% after removing the necrotic parts of specimens [28] (see Methods). Six of the samples were radiation-naïve, newly diagnosed HGG (WHO grade IV or GBM). One sample was a recurrent and irradiated anaplastic astrocytoma (WHO grade III) (Supplemental Table 2). However, this tumor clinically behaved like a grade IV GBM, with rapid progression and resistance to multiple therapies. We, therefore, suspect that the histologic diagnosis may have underestimated tumor grade due to sampling bias. All samples were wild-type for IDH1. Six of the seven specimens were subjected to DNA methylation analysis with 450K arrays, which allow molecular subtyping [34]. Based on DNA methylation, one tumor was classified as proneural (RTK1) GBM, whereas the rest were classified as non-RTK1 GBM, which signifies either classical (RTK2) or mesenchymal subtype [3]. The DNA methylation analysis also showed distinct copy number variation profiles for each sample, demonstrating the molecular intertumoral heterogeneity of HGG (Supplemental Figure 1). In four specimens, the MGMT promoter was methylated. The three MGMT-unmethylated specimens showed epidermal growth factor receptor amplification. One of the HGG samples contained sarcomatous features by histology (Supplemental Table 2). These data suggest that, despite the small sample size used in this study, the explant cultures generated represent a highly heterogeneous population of HGG samples, with variable mutational make-ups.

To generate explant cultures, fresh surgical specimens were dissected, and multiple fragments were placed on laminin-coated filters in the upper chamber of Transwell inserts (Figure 2*A*). Explants were cultured for 4 days prior to analysis. During this time, the specimens flattened, allowing easier diffusion of RIKI. Supplemental Table 3 summarizes the conditions used and the experiments performed with each patient sample.

We assessed the TGF-β responsiveness and efficacy of inhibition by LY364947 (RIKI). In cell-free assays, LY364947 inhibits TGFβRI (ALK5) with an IC_{50} of 0.58 μM [42], but nonspecific effects on other kinases have been demonstrated [43]. RIKI has been used at concentrations ranging from 0.4 to 10 μM in cell-based assays [8,44,45]. Because drug bioavailability deep within explants cannot be predicted by previous *in vitro* assays, we tested two concentrations of RIKI (0.4 μM and 2 μM; 24-hour treatment) in six explants using immunofluorescence analysis for nuclear p-Smad2. In keeping with the reported characterization of the compound, the low concentration of RIKI had little effect (data not shown), whereas 2 μM RIKI given for 24 hours effectively blocked TGF-β induction of p-Smad2 (representative images from L46, Figure 2*B*). The fraction of p-Smad2+ cells after TGF-β and RIKI (24 hours) treatments of individual specimens was variable (Supplemental Figure 2); thus, the data were normalized to their respective controls. Although RIKI (2 μM) alone did not affect baseline p-Smad2 immunoreactivity, the fraction of cells positive for nuclear p-Smad2 increased 1.56 ± 0.09-fold upon exposure to exogenous TGF-β for 30 minutes ($P < 0.05$), indicating that HGGs were responsive to TGF-β (Figure 2*C*). The fraction of TGF-β–treated cells positive for nuclear p-Smad2 decreased 1.75 ± 0.12-fold by 24-hour pretreatment with 2 μM RIKI compared with TGF-β alone ($P < 0.01$) (Figure 2*C*), suggesting efficient inhibition of TGF-β signaling by RIKI. Overall, these findings indicate that RIKI blocks TGF-β–induced phosphorylation of Smad2 in HGG explants and suggest that explant cultures are an effective model system to study the effects of small molecular inhibitors *ex vivo*.

Impaired Recognition of Radiation-Induced DNA Damage by Inhibition of TGF-β Signaling

The histone H2AX becomes phosphorylated (γ-H2AX) in chromatin localizing to DSB [46]. The resulting foci of γ-H2AX serve as a means to evaluate cellular efficacy of DSB recognition and DDR [47,48]. Inhibition of TGF-β signaling leads to decreased formation of γ-H2AX foci and reduced cell survival in irradiated GBM cell lines [8], suggesting TGF-β is required for recognition of DSB and effective DDR. Having confirmed that RIKI efficiently blocks activation of TGF-β signaling in HGG explants, we tested its effects on the response to IR in these specimens. Explant cultures were incubated with RIKI for 24 hours prior to irradiation with 2 Gy, which represents a single fraction of the dose HGG patients receive for therapy (Figure 3*A*).

Radiation induces TGF-β activation, which is evident as p-Smad2 induction [49]. To confirm that radiation elicits TGF-β activation in HGG explants, we quantified the percentage of p-Smad2+ cells in explants from specimen L50 under control conditions (sham), in the presence of RIKI, 60 minutes after IR, and after combined IR and RIKI (Figure 3*B*). RIKI completely abolished the radiation-induced increase in the fraction of p-Smad2+ cells. This finding, combined with the fact that RIKI blocks the TGF-β–induced increase in the fraction of p-Smad2+ cells (Figure 2, *B* and *C*), suggests that irradiation of explant cultures upregulates TGF-β signaling and that RIKI is an effective blocker of this signaling pathway.

IR increased the percentage of γ-H2AX+ nuclei, defined as those with one or more foci, across explant specimens, and RIKI did not affect the percentage of γ-H2AX+ cells (Supplemental Figure 3*A*). Given that all cells are damaged by IR, we were puzzled by the fact that certain cells lacked radiation-induced γ-H2AX foci. We determined that the percentage of γ-H2AX+ cells did not correlate with the number of γ-H2AX foci per nucleus in irradiated cultures (Supplemental Figure 3*B*). We noted that γ-H2AX– nuclei were

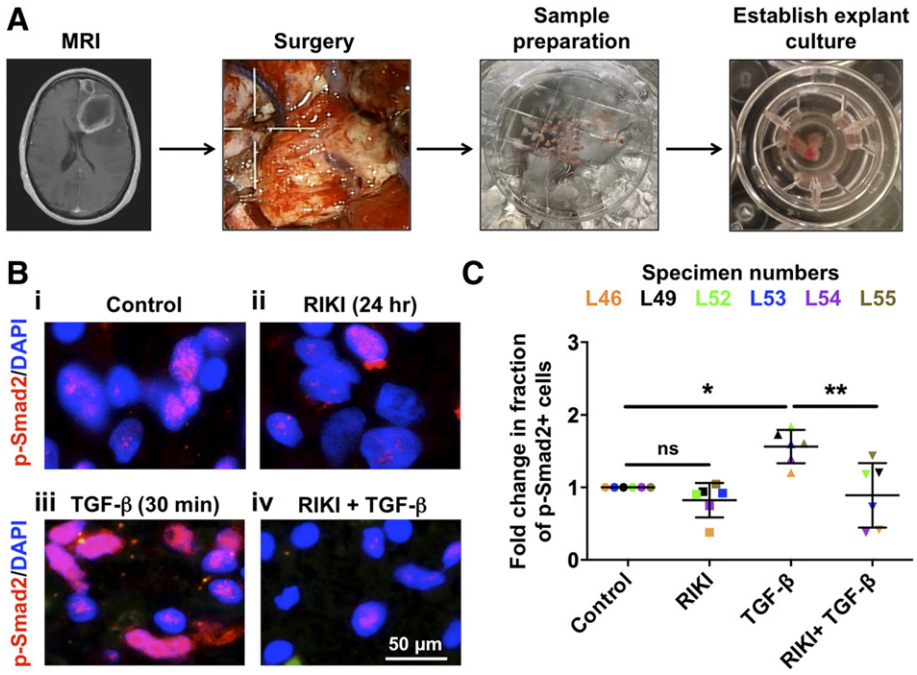

Figure 2. Establishment of HGG cultures and effects of RIKI on TGF-β–induced Smad2 phosphorylation. (A) Schematic showing the establishment of cultures from surgical HGG specimens. (B) Representative images of p-Smad2 (red) immunofluorescence analysis (specimen L46) at baseline (i), after 24 hours of RIKI (ii), after 30 minutes of TGF-β (iii), and after combined RIKI and TGF-β (iv). Nuclei are counterstained with DAPI (blue). RIKI was given for 24 hours and TGF-β for 30 minutes prior to assays. (C) The fraction of p-Smad2–positive cells increased after TGF-β stimulation in GBM cultures. This effect was blocked by pretreatment with RIKI. The mean values and standard error of six specimens are shown [AVOVA $F_{(3,20)} = 8.876$, $P = 0.006$]. *$P < 0.05$; **$P < 0.01$.

substantially smaller than their γ-H2AX+ counterparts, raising the possibility that they were not tumor cells (Supplemental Figure 3*C*). We tested the idea that these cells were bone marrow–derived or putative tumor stem cells but found that the negative cells were neither CD45+ leukocytes [50–52] nor Sox2+ GSCs [8,31]; indeed, γ-H2AX foci colocalized with both markers, which provided a qualitative demonstration that both leukocytes and GSCs responded to IR with induction of γ-H2AX foci (Supplemental Figure 3*D*). Based on these considerations, we eliminated negative cells from quantification of the radiation response.

Thus, to assess radiation sensitivity, we evaluated only cells with γ-H2AX foci and enumerated the number of foci per nucleus, which is reported to reach the maximum number within the first hour after IR, at the 30- and 60-minutes marks. The number of γ-H2AX foci increased following IR, and this was abolished with RIKI treatment (representative images from L46, Figure 3*C*). We used quantitative image analysis to determine the number of nuclear γ-H2AX foci (Figure 3*D*), as previously described [38,53]. RIKI did not affect the number of γ-H2AX foci per nucleus in the absence of radiation (Figure 3, *E* and *F*). At 30 minutes, the mean number of foci per nucleus increased from 2.5 ± 0.2 to 9.9 ± 0.8 ($n = 6$ explants), and at 60 minutes, the mean value was 10.5 ± 1.5 ($n = 7$ explants). Pretreatment of irradiated explants with RIKI reduced the number of γ-H2AX foci per nucleus at both the 30-minute (6.5 ± 0.9) and the 60-minute (6.3 ± 0.9) marks. These data suggest that TGF-β inhibition impairs formation of γ-H2AX foci in HGG explants, in line with our previous data [8].

RIKI Prevents Radiation-Induced Upregulation of Sox2

Our previous work indicated that radiation enhances GSC self-renewal, as evidenced by increased expression of transcription factor Sox2, a GSC marker [31], and *in vitro* tumorsphere formation, in the murine GBM cell line GL261 [8]. Hence, we tested if radiation leads to increased levels of Sox2 in HGG explants and if TGF-β signaling blockade with RIKI affects this response. Specimens were analyzed at 60 minutes post-radiation using immunofluorescence to detect Sox2. The degree of Sox2 expression varied across explants (Supplemental Figure 4). We observed an increase in nuclear Sox2 immunofluorescence after radiation, and this increase was blocked by 24-hour pretreatment with RIKI (representative images from L52, Figure 4*A*). Cumulatively, irradiated specimens showed a 2.4 ± 0.3-fold increase in the intensity of nuclear Sox2 immunofluorescence compared with no radiation ($n = 6$) (Figure 4*B*). RIKI prevented upregulation of nuclear Sox2 intensity after radiation ($n = 6$). Interestingly, two explants did not follow this overall response pattern for different reasons. Radiation had no effect on Sox2 immunofluorescence in specimen L54, wherease RIKI failed to suppress the radiation-induced increase in Sox2 levels in L55. These results suggest that radiation-induced upregulation of Sox2, a transcription factor implicated in GSC self-renewal, requires TGF-β signaling.

Personalized Screening of TGF-β Inhibition Using Irradiated HGG Explant Cultures

Cumulative statistics from the seven HGG explant cultures showed that RIKI reduced radiation-induced γ-H2AX foci (Figure 3, *D* and *E*).

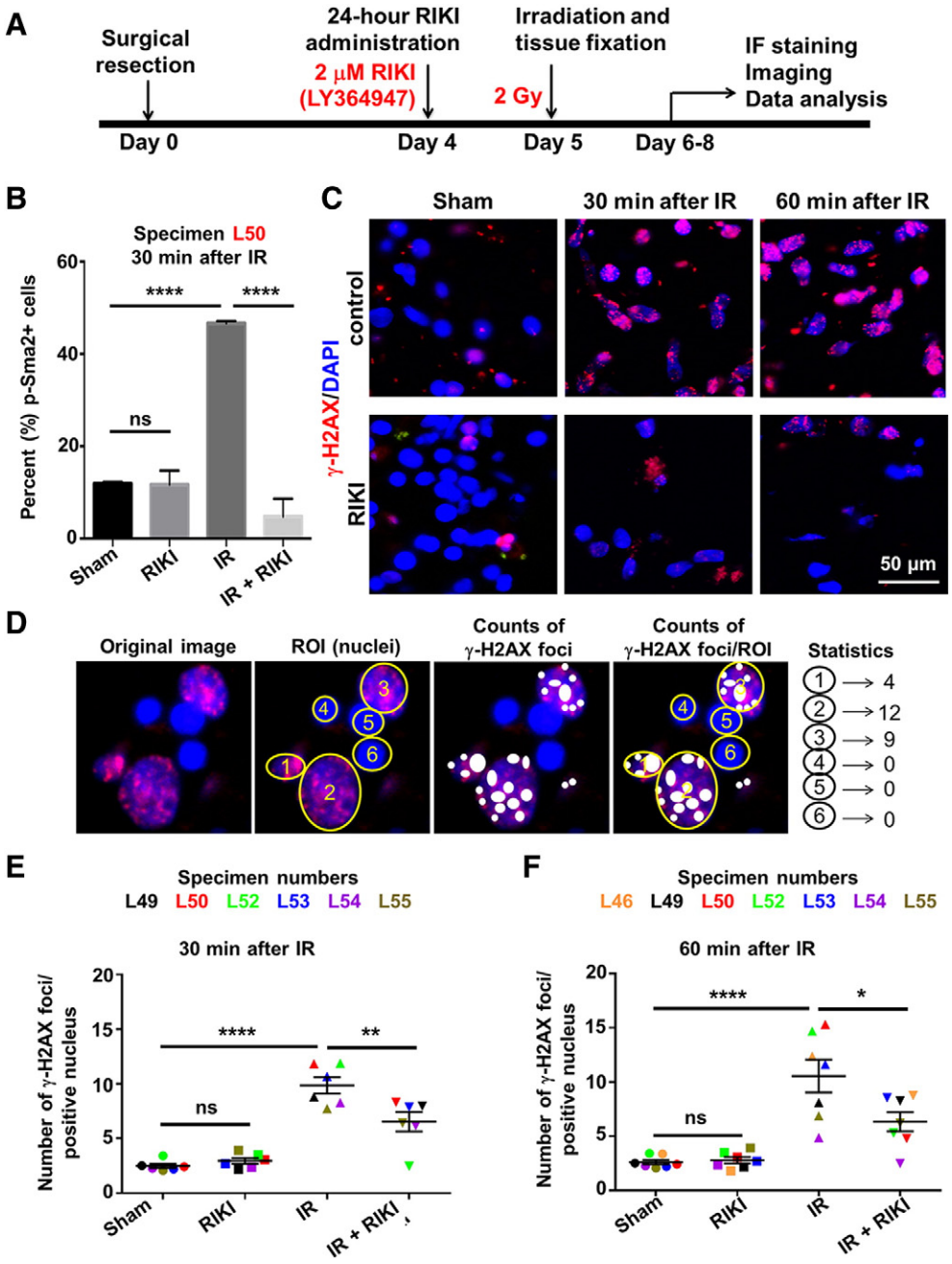

Figure 3. DSB recognition dynamics in HGG explant cultures analyzed by γ-H2AX immunoreactivity. (A) Experimental timeline for testing radiosensitizing effects of TGF-β inhibition. (B) RIKI prevented the radiation-induced increase in the percentage of p-Smad2+ cells in explants from specimen L50. RIKI had no effect on the fraction of p-Smad2+ cells in the absence of radiation [ANOVA $F_{(3,8)} = 170.3$, $P < 0.0001$]. (C) Representative images of effects of RIKI on γ-H2AX (red) immunofluorescence (specimen L46) before and after radiation. Nuclei are counterstained with DAPI (blue). (D) Schematic representation of quantitation of γ-H2AX foci. Only the positive nuclei were considered for analysis. (E) Cumulative data for γ-H2AX foci/positive nucleus in six explants 30 minutes after radiation [ANOVA $F_{(3,20)} = 32.38$, $P < 0.0001$]. (F) Collective data for γ-H2AX foci/positive nucleus in seven explants 60 minutes after irradiation [ANOVA $F_{(3,24)} = 17.44$, $P < 0.0001$]. *ns*, not significant. *$P < 0.05$; **$P < 0.01$; ****$P < 0.0001$.

However, based on the response of individual HGG explants, two categories were evident: five responders that showed decreased γ-H2AX foci upon RIKI treatment (Figure 5, *Ai–v*) and two nonresponders (Figure 5, *Bi* and *ii*). This dichotomy was evident at both 30 and 60 minutes after radiation. The two nonresponder explants had these properties: In L49, RIKI suppressed Sox2 upregulation by radiation but not the increase in γ-H2AX foci (Figure 5*Bi*, Supplemental Figure 4). L55 failed to show effects of RIKI on formation of γ-H2AX foci, much like it failed to show prevention of Sox2 upregulation by RIKI (Figure 5*Bii*, Supplemental Figure 4). Finally, L54 showed induction of γ-H2AX foci by radiation and their suppression by RIKI but did not demonstrate increased radiation-induced Sox2 expression (Figure 5Bi, Supplemental Figure 4). There was no obvious correlation between the

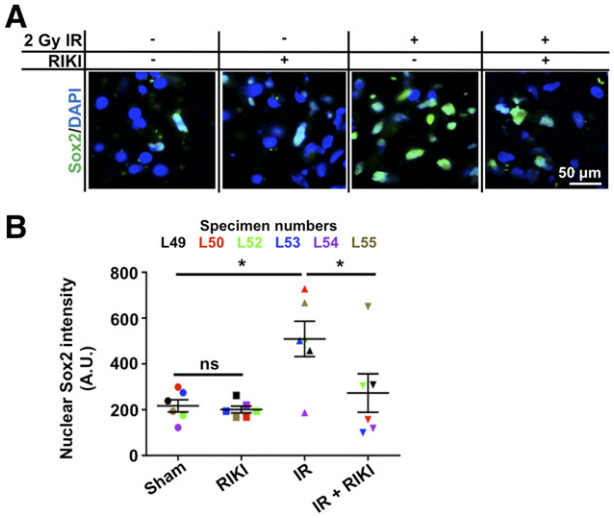

Figure 4. Inhibition of TGF-β signaling prevents radiation-induced upregulation of GSC marker Sox2. (A) Representative images showing effects of RIKI on Sox2 immunostaining (green) before and after radiation (specimen L52). Nuclei were counterstained with DAPI (blue). (B) Nuclear Sox2 intensity at 60 minutes after 2-Gy irradiation in six HGG explant cultures [ANOVA $F_{(3,20)} = 5.837$, $P = 0.0049$]. *$P < 0.05$.

molecular subtype of the explants or their baseline p-Smad2 levels and their response pattern in this small cohort of samples. These results demonstrate that the response to TGF-β inhibition in the context of radiotherapy varies among tumors, highlighting the need for personalized approaches.

Discussion

One of the main roadblocks in HGG research is the lack of experimental models recapitulating the extensive intertumoral heterogeneity of the disease [3,4]. It is now clear that the "one size fits all" approach to treatment is unlikely to succeed because of this heterogeneity and that understanding the biological properties of individual tumors will provide paths to personalized therapy. However, some of the personalized therapy approaches, such as high-throughput next-generation sequencing, may not always be cost-and time-efficient and do not provide functional data. Patient-derived cultures and xenografts certainly capture individual tumor properties, but developing and testing these models are nonetheless lengthy and laborious. Importantly, *in vitro* cultures and xenografts in immunocompromised mice do not take into account the full range of cells that make up the TME. Explant cultures represent an effective alternative to such models. Not only can they can be subjected to testing within hours to days after tissue procurement, but they also preserve the tissue architecture and interactions of tumor cells with the microenvironment to provide the appropriate biological context for assessing basic tumor biology and response to treatment. Indeed, explant cultures have been previously used successfully to study HGGs [28–30].

TGF-β and components of its signaling pathway are highly expressed in HGG and are linked to GSC self-renewal [10–13,20]. Moreover, previous studies have indicated that radiation enriches GSCs in HGG [7,15], that GSC *in vitro* surrogates produce abundant TGF-β [8], and that radiation therapy activates TGF-β [21,49]. Our prior experiments showed that inhibition of TGFβR1 kinase activity with RIKI impedes recognition of radiation-induced DNA damage and suppresses induction of self-renewal signals associated with tumorsphere-forming cells (an *in vitro* surrogate of GSCs) in a GBM cell line [8]. Interference with these radiation responses results in decreased clonogenic survival and improved tumor response in a subcutaneous brain tumor model [8], as well as in breast [54] and lung [55] tumor models. Our current study aimed to extend our previous findings and test the role of TGF-β in HGG radioresistance in human HGG tissue.

Accurate and efficient DDR of cancer cells is often compromised, which is considered an Achilles heel that can be targeted to achieve better response to therapies [56]. Here, we used explant cultures to study the effects of TGF-β inhibition on radioresponse and DDR in HGG. First, we interrogated the TCGA for expression levels of transcripts related to TGF-β signaling and found differences among molecular subtypes of GBM. Second, we immunostained 14 human HGG FFPE specimens for p-Smad2 and confirmed that the extent of TGF-β signaling pathway activation is variable across tumors, similar to prior observations [20]. Using HGG explants, we found that inhibition of TGF-β receptor I with RIKI reduces the number of γ-H2AX foci after radiation, suggesting attenuation of the tumor's response to DNA damage. Even more importantly, this radiosensitizing effect of RIKI was observed in five of seven specimens but was absent in the two other specimens. This heterogeneous response to RIKI was in agreement with our analysis of TCGA data and immunostaining of FFPE biospecimens for p-Smad2. We conclude that the explant method can distinguish tumors with differential sensitivity to TGF-β inhibition in the context of radioresponse [57] and establishes a proof-of-concept paradigm for patient-specific screening of candidate therapies. Furthermore, the predicted benefit of TGF-β inhibition in most HGGs provides further motivation for their current clinical testing but also underscores the utility of implementing *ex vivo* assays for personalized efficacy studies.

In addition to the significant effects of IR and RIKI on the number of γ-H2AX foci/nucleus, we observed that not all cells in the HGG explants responded to radiation and that the percentage of γ-H2AX+ cells remained variable across samples, without any correlation to the number of γ-H2AX foci/nucleus. We demonstrated that CD45+ tumor leukocytes and Sox2+ GSCs both respond to IR with induction of γ-H2AX foci. The nature of the γ-H2AX- cells remains unknown at this point and requires future investigation. The fact that γ-H2AX- cells have smaller nuclei leads us to speculate that they may represent normal brain cells or other cellular components of the TME, which may exhibit different dynamics of DSB recognition and DRR from tumor cells.

Previous clinical trials with TGF-β receptor I inhibitor or antisense oligonucleotide against TGF-β2 in recurrent post-radiation HGG showed mixed results, with favorable responses only in a subset of patients [25–27], especially those harboring IDH1 mutations in their tumors [25,26]. Our explant culture findings suggest that TGF-β inhibition may be efficacious in subsets of radiation-naïve HGG patients and provide rationale for designing additional clinical trials testing the efficacy of TGF-β inhibitors in newly diagnosed HGG, while highlighting the need for patient screening and stratification. Furthermore, the explant system represents an ideal platform for comparing the effect of TGF-β inhibition on radioresponse in IDH1-mutated and IDH1–wild-type tumors in the future.

The evidence that TME is an important regulator of radioresponse emphasizes the need to develop novel testing platforms to test

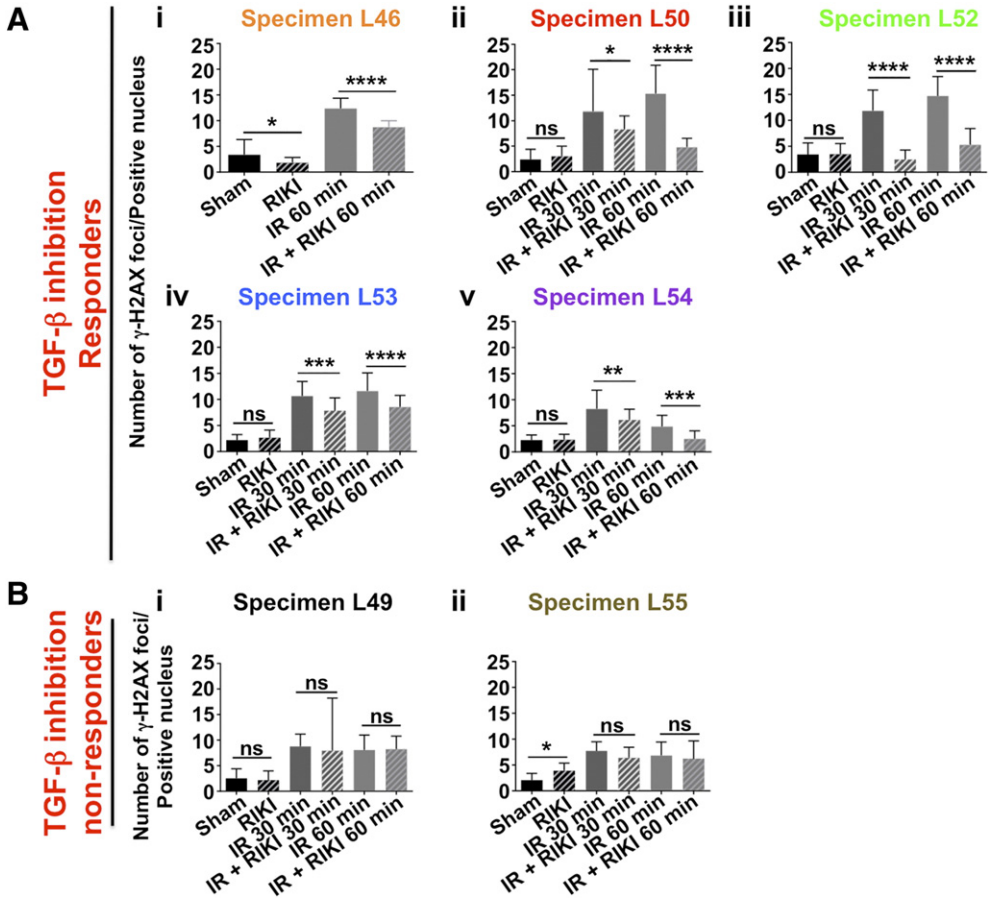

Figure 5. The response to TGF-β inhibition varies among different specimens. (Ai-v) Five explants responded to RIKI with decreases in radiation-induced γ-H2AX foci. (i) L46 [ANOVA $F_{(3116)} = 186.9$, $P < 0.0001$]. (ii) L50 [ANOVA $F_{(5174)} = 41.49$, $P < 0.0001$]. (iii) L52 [ANOVA $F_{(5174)} = 91.12$, $P < 0.0001$]. (iv) L53 [ANOVA $F_{(5174)} = 84.59$, $P < 0.0001$]. (v) L54 [ANOVA $F_{(5174)} = 43.16$, $P < 0.0001$]. (Bi-ii) In two explants, RIKI did not suppress radiation-induced γ-H2AX foci. (i) L49 [ANOVA $F_{(5174)} = 12.93$, $P < 0.0001$]. (ii) L55 [ANOVA $F_{(5174)} = 27.70$, $P < 0.0001$]. *$P < 0.05$; **$P < 0.01$; ***$P < 0.001$; ****$P < 0.0001$.

putative radiosensitizers [15,58]. Although orthotopic tumor xenografts in the mouse brain provide a suitable model for testing drugs in an appropriate microenvironmental context, drug assays become logistically challenging *in vivo*. Furthermore, the fact that xenografts are implants in immunocompromised mice implies that immune components of the TME are lacking. The use of *ex vivo* systems to test the effect of IR in conjunction with candidate radiosensitizing agents preserves human microenvironmental factors without the logistical limitation of performing such assays in orthotopic xenografts. Additionally, the potential to evaluate individual patient samples allows for personalized patient-specific biological assays in the setting of a highly heterogeneous tumor type. Finally, the concept of explant cultures, once technically refined, appears theoretically amenable to high-throughput screening of chemical libraries, which is not feasible with *in vivo* testing. In the future, we envision that this platform could be used to individually test FDA-approved drugs toward the establishment of personalized therapy regimens.

Conclusions

Inhibition of TGF-β signaling with a small molecule inhibitor of the kinase activity of TGF-β receptor I attenuates recognition of radiation-induced DSB and expression of the GSC marker Sox2 in most, but not all, HGG explant cultures. Our findings indicate the general utility of TGF-β inhibition as a radiosensitization approach but also underscore the heterogeneity in the response of individual tumors. We propose that HGG explant cultures can be used to test individual tumors for effects of TGF-β inhibitors on radioresponse, and more generally, as a flexible *ex vivo* platform for screening drugs with antitumor activity in patient-specific fashion.

Acknowledgements

The authors thank Mr. William Chou for technical assistance. The results shown in Figure 1 are based upon data generated by the TCGA Research Network (http://cancergenome.nih.gov/). This research was supported by the National Institutes of Health (1R21NS088775-01 to D.G.P. and M.H.B.-H). N. S. B. received support from NYSTEM Institutional training grant #CO26880.

Appendix A. Supplementary Data

Supplementary data to this article can be found online at http://dx.doi.org/10.1016/j.neo.2016.08.008.

References

[1] Stupp R, Mason WP, van den Bent MJ, Weller M, Fisher B, Taphoorn MJ, Belanger K, Brandes AA, Marosi C, and Bogdahn U, et al (2005). Radiotherapy plus concomitant and adjuvant temozolomide for glioblastoma. *N Engl J Med* **352**, 987–996.

[2] Gilbert MR, Dignam JJ, Armstrong TS, Wefel JS, Blumenthal DT, Vogelbaum MA, Colman H, Chakravarti A, Pugh S, and Won M, et al (2014). A randomized trial of bevacizumab for newly diagnosed glioblastoma. *N Engl J Med* **370**, 699–708.

[3] Verhaak RG, Hoadley KA, Purdom E, Wang V, Qi Y, Wilkerson MD, Miller CR, Ding L, Golub T, and Mesirov JP, et al (2010). Integrated genomic analysis identifies clinically relevant subtypes of glioblastoma characterized by abnormalities in PDGFRA, IDH1, EGFR, and NF1. *Cancer Cell* **17**, 98–110.

[4] Eckel-Passow JE, Lachance DH, Molinaro AM, Walsh KM, Decker PA, Sicotte H, Pekmezci M, Rice T, Kosel ML, and Smirnov IV, et al (2015). Glioma groups based on 1p/19q, IDH, and TERT promoter mutations in tumors. *N Engl J Med* **372**, 2499–2508.

[5] Singh SK, Hawkins C, Clarke ID, Squire JA, Bayani J, Hide T, Henkelman RM, Cusimano MD, and Dirks PB (2004). Identification of human brain tumour initiating cells. *Nature* **432**, 396–401.

[6] Chen J, Li Y, Yu TS, McKay RM, Burns DK, Kernie SG, and Parada LF (2012). A restricted cell population propagates glioblastoma growth after chemotherapy. *Nature* **488**, 522–526.

[7] Bao S, Wu Q, McLendon RE, Hao Y, Shi Q, Hjelmeland AB, Dewhirst MW, Bigner DD, and Rich JN (2006). Glioma stem cells promote radioresistance by preferential activation of the DNA damage response. *Nature* **444**, 756–760.

[8] Hardee ME, Marciscano AE, Medina-Ramirez CM, Zagzag D, Narayana A, Lonning SM, and Barcellos-Hoff MH (2012). Resistance of glioblastoma-initiating cells to radiation mediated by the tumor microenvironment can be abolished by inhibiting transforming growth factor-beta. *Cancer Res* **72**, 4119–4129.

[9] Wang J, Wakeman TP, Lathia JD, Hjelmeland AB, Wang XF, White RR, Rich JN, and Sullenger BA (2010). Notch promotes radioresistance of glioma stem cells. *Stem Cells* **28**, 17–28.

[10] Zhang M, Kleber S, Rohrich M, Timke C, Han N, Tuettenberg J, Martin-Villalba A, Debus J, Peschke P, and Wirkner U, et al (2011). Blockade of TGF-beta signaling by the TGFbetaR-I kinase inhibitor LY2109761 enhances radiation response and prolongs survival in glioblastoma. *Cancer Res* **71**, 7155–7167.

[11] Penuelas S, Anido J, Prieto-Sanchez RM, Folch G, Barba I, Cuartas I, Garcia-Dorado D, Poca MA, Sahuquillo J, and Baselga J, et al (2009). TGF-beta increases glioma-initiating cell self-renewal through the induction of LIF in human glioblastoma. *Cancer Cell* **15**, 315–327.

[12] Ikushima H, Todo T, Ino Y, Takahashi M, Miyazawa K, and Miyazono K (2009). Autocrine TGF-beta signaling maintains tumorigenicity of glioma-initiating cells through Sry-related HMG-box factors. *Cell Stem Cell* **5**, 504–514.

[13] Anido J, Saez-Borderias A, Gonzalez-Junca A, Rodon L, Folch G, Carmona MA, Prieto-Sanchez RM, Barba I, Martinez-Saez E, and Prudkin L, et al (2010). TGF-beta receptor inhibitors target the CD44(high)/Id1(high) glioma-initiating cell population in human glioblastoma. *Cancer Cell* **18**, 655–668.

[14] Wick W, Platten M, and Weller M (2001). Glioma cell invasion: regulation of metalloproteinase activity by TGF-beta. *J Neurooncol* **53**, 177–185.

[15] Jamal M, Rath BH, Tsang PS, Camphausen K, and Tofilon PJ (2012). The brain microenvironment preferentially enhances the radioresistance of CD133(+) glioblastoma stem-like cells. *Neoplasia* **14**, 150–158.

[16] Joseph JV, Balasubramaniyan V, Walenkamp A, and Kruyt FA (2013). TGF-beta as a therapeutic target in high grade gliomas — promises and challenges. *Biochem Pharmacol* **85**, 478–485.

[17] Platten M, Wick W, and Weller M (2001). Malignant glioma biology: role for TGF-beta in growth, motility, angiogenesis, and immune escape. *Microsc Res Tech* **52**, 401–410.

[18] Caja L, Bellomo C, and Moustakas A (2015). Transforming growth factor beta and bone morphogenetic protein actions in brain tumors. *FEBS Lett* **589**, 1588–1597.

[19] Roy LO, Poirier MB, and Fortin D (2015). Transforming growth factor-beta and its implication in the malignancy of gliomas. *Target Oncol* **10**, 1–14.

[20] Bruna A, Darken RS, Rojo F, Ocana A, Penuelas S, Arias A, Paris R, Tortosa A, Mora J, and Baselga J, et al (2007). High TGFbeta-Smad activity confers poor prognosis in glioma patients and promotes cell proliferation depending on the methylation of the PDGF-B gene. *Cancer Cell* **11**, 147–160.

[21] Dancea HC, Shareef MM, and Ahmed MM (2009). Role of radiation-induced TGF-beta signaling in cancer therapy. *Mol Cell Pharmacol* **1**, 44–56.

[22] Massague J (2012). TGFbeta signalling in context. *Nat Rev Mol Cell Biol* **13**, 616–630.

[23] Zhang M, Herion TW, Timke C, Han N, Hauser K, Weber KJ, Peschke P, Wirkner U, Lahn M, and Huber PE (2011). Trimodal glioblastoma treatment consisting of concurrent radiotherapy, temozolomide, and the novel TGF-β receptor I kinase inhibitor LY2109761. *Neoplasia* **13**, 537–549.

[24] Zhang M, Lahn M, and Huber PE (2012). Translating the combination of TGFbeta blockade and radiotherapy into clinical development in glioblastoma. *Oncoimmunology* **1**, 943–945.

[25] Rodon J, Carducci MA, Sepulveda-Sanchez JM, Azaro A, Calvo E, Seoane J, Brana I, Sicart E, Gueorguieva I, and Cleverly AL, et al (2015). First-in-human dose study of the novel transforming growth factor-beta receptor I kinase inhibitor LY2157299 monohydrate in patients with advanced cancer and glioma. *Clin Cancer Res* **21**, 553–560.

[26] Brandes AA, Carpentier AF, Kesari S, Sepulveda-Sanchez JM, Wheeler HR, Chinot O, Cher L, Steinbach JP, Capper D, and Specenier P, et al (2016). A phase II randomized study of galunisertib monotherapy or galunisertib plus lomustine compared with lomustine monotherapy in patients with recurrent glioblastoma. *Neuro Oncol* **18**, 1146–1156.

[27] Bogdahn U, Hau P, Stockhammer G, Venkataramana NK, Mahapatra AK, Suri A, Balasubramaniam A, Nair S, Oliushine V, and Parfenov V, et al (2011). Targeted therapy for high-grade glioma with the TGF-beta2 inhibitor trabedersen: results of a randomized and controlled phase IIb study. *Neuro Oncol* **13**, 132–142.

[28] Shimizu F, Hovinga KE, Metzner M, Soulet D, and Tabar V (2011). Organotypic explant culture of glioblastoma multiforme and subsequent single-cell suspension. *Curr Protoc Stem Cell Biol* [**chapter 3**, unit3 5].

[29] Hovinga KE, Shimizu F, Wang R, Panagiotakos G, Van Der Heijden M, Moayedpardazi H, Correia AS, Soulet D, Major T, and Menon J, et al (2010). Inhibition of notch signaling in glioblastoma targets cancer stem cells via an endothelial cell intermediate. *Stem Cells* **28**, 1019–1029.

[30] Merz F, Gaunitz F, Dehghani F, Renner C, Meixensberger J, Gutenberg A, Giese A, Schopow K, Hellwig C, and Schafer M, et al (2013). Organotypic slice cultures of human glioblastoma reveal different susceptibilities to treatments. *Neuro Oncol* **15**, 670–681.

[31] Ben-Porath I, Thomson MW, Carey VJ, Ge R, Bell GW, Regev A, and Weinberg RA (2008). An embryonic stem cell–like gene expression signature in poorly differentiated aggressive human tumors. *Nat Genet* **40**, 499–507.

[32] Xie W, Aisner S, Baredes S, Sreepada G, Shah R, and Reiss M (2013). Alterations of Smad expression and activation in defining 2 subtypes of human head and neck squamous cell carcinoma. *Head Neck* **35**, 76–85.

[33] Zagzag D, Krishnamachary B, Yee H, Okuyama H, Chiriboga L, Ali MA, Melamed J, and Semenza GL (2005). Stromal cell–derived factor-1alpha and CXCR4 expression in hemangioblastoma and clear cell-renal cell carcinoma: von Hippel–Lindau loss-of-function induces expression of a ligand and its receptor. *Cancer Res* **65**, 6178–6188.

[34] Sturm D, Witt H, Hovestadt V, Khuong-Quang DA, Jones DT, Konermann C, Pfaff E, Tonjes M, Sill M, and Bender S, et al (2012). Hotspot mutations in H3F3A and IDH1 define distinct epigenetic and biological subgroups of glioblastoma. *Cancer Cell* **22**, 425–437.

[35] Assenov Y, Muller F, Lutsik P, Walter J, Lengauer T, and Bock C (2014). Comprehensive analysis of DNA methylation data with RnBeads. *Nat Methods* **11**, 1138–1140.

[36] Triche Jr TJ, Weisenberger DJ, Van Den Berg D, Laird PW, and Siegmund KD (2013). Low-level processing of Illumina Infinium DNA Methylation BeadArrays. *Nucleic Acids Res* **41**, e90.

[37] Teschendorff AE, Marabita F, Lechner M, Bartlett T, Tegner J, Gomez-Cabrero D, and Beck S (2013). A beta-mixture quantile normalization method for correcting probe design bias in Illumina Infinium 450k DNA methylation data. *Bioinformatics* **29**, 189–196.

[38] Costes SV, Boissiere A, Ravani SA, Romano R, Parvin B, and Barcellos-Hoff MH (2006). Imaging features that discriminate between high and low LET radiation-induced foci in human fibroblasts. *Radiat Res* **165**, 505–515.

[39] Sivasankaran B, Degen M, Ghaffari A, Hegi ME, Hamou MF, Ionescu MC, Zweifel C, Tolnay M, Wasner M, and Mergenthaler S, et al (2009). Tenascin-C is a novel RBPJkappa-induced target gene for Notch signaling in gliomas. *Cancer Res* **69**, 458–465.

[40] Phillips GR, Krushel LA, and Crossin KL (1998). Domains of tenascin involved in glioma migration. *J Cell Sci* **111**(Pt 8), 1095–1104.

[41] Hau P, Kunz-Schughart LA, Rummele P, Arslan F, Dorfelt A, Koch H, Lohmeier A, Hirschmann B, Muller A, and Bogdahn U, et al (2006). Tenascin-C protein is induced by transforming growth factor-beta1 but does not correlate with time to tumor progression in high-grade gliomas. *J Neurooncol* **77**, 1–7.

[42] Peng SB, Yan L, Xia X, Watkins SA, Brooks HB, Beight D, Herron DK, Jones ML, Lampe JW, and McMillen WT, et al (2005). Kinetic characterization of novel pyrazole TGF-beta receptor I kinase inhibitors and their blockade of the epithelial-mesenchymal transition. *Biochemistry* **44**, 2293–2304.

[43] Vogt J, Traynor R, and Sapkota GP (2011). The specificities of small molecule inhibitors of the TGFss and BMP pathways. *Cell Signal* **23**, 1831–1842.

[44] Jaskova K, Pavlovicova M, Cagalinec M, Lacinova L, and Jurkovicova D (2014). TGFbeta1 downregulates neurite outgrowth, expression of Ca2+ transporters, and mitochondrial dynamics of in vitro cerebellar granule cells. *Neuroreport* **25**, 340–346.

[45] Dhasarathy A, Phadke D, Mav D, Shah RR, and Wade PA (2011). The transcription factors Snail and Slug activate the transforming growth factor-beta signaling pathway in breast cancer. *PLoS One* **6**, e26514.

[46] Kuo LJ and Yang LX (2008). Gamma-H2AX — a novel biomarker for DNA double-strand breaks. *In Vivo* **22**, 305–309.

[47] Kinner A, Wu W, Staudt C, and Iliakis G (2008). Gamma-H2AX in recognition and signaling of DNA double-strand breaks in the context of chromatin. *Nucleic Acids Res* **36**, 5678–5694.

[48] Cucinotta FA, Pluth JM, Anderson JA, Harper JV, and O'Neill P (2008). Biochemical kinetics model of DSB repair and induction of gamma-H2AX foci by non-homologous end joining. *Radiat Res* **169**, 214–222.

[49] Barcellos-Hoff MH, Derynck R, Tsang ML, and Weatherbee JA (1994). Transforming growth factor-beta activation in irradiated murine mammary gland. *J Clin Invest* **93**, 892–899.

[50] Hussain SF, Yang D, Suki D, Aldape K, Grimm E, and Heimberger AB (2006). The role of human glioma-infiltrating microglia/macrophages in mediating antitumor immune responses. *Neuro Oncol* **8**, 261–279.

[51] Du R, Lu KV, Petritsch C, Liu P, Ganss R, Passegue E, Song H, Vandenberg S, Johnson RS, and Werb Z, et al (2008). HIF1alpha induces the recruitment of bone marrow–derived vascular modulatory cells to regulate tumor angiogenesis and invasion. *Cancer Cell* **13**, 206–220.

[52] Strik HM, Stoll M, and Meyermann R (2004). Immune cell infiltration of intrinsic and metastatic intracranial tumours. *Anticancer Res* **24**, 37–42.

[53] Groesser T, Chang H, Fontenay G, Costes SV, Chen J, Barcellos-Hoff MH, Parvin B, and Rydberg B (2011). Persistence of g-H2AX and 53BP1 foci in proliferating and non-proliferating human mammary epithelial cells after exposure to g-rays or iron ions. *Int J Radiat Biol* **87**, 696–710.

[54] Bouquet SF, Pal A, Pilones KA, Demaria S, Hann B, Akhurst RJ, Babb JS, Lonning SM, DeWyngaert JK, and Formenti S, et al (2011). Transforming growth factor β1 inhibition increases the radiosensitivity of breast cancer cells *in vitro* and promotes tumor control by radiation *in vivo*. *Clin Cancer Res* **17**, 6754–6765.

[55] Du S, Bouquet F, Lo C-H, Pellicciotta I, Bolourchi S, Parry R, and Barcellos-Hoff MH (2014). Attenuation of the DNA damage response by TGFβ inhibitors enhances radiation sensitivity of NSCLC cells in vitro and in vivo. *Int J Radiat Oncol Biol Phys* **91**, 91–99.

[56] Farmer H, McCabe N, Lord CJ, Tutt AN, Johnson DA, Richardson TB, Santarosa M, Dillon KJ, Hickson I, and Knights C, et al (2005). Targeting the DNA repair defect in BRCA mutant cells as a therapeutic strategy. *Nature* **434**, 917–921.

[57] Menegakis A, De Colle C, Yaromina A, Hennenlotter J, Stenzl A, Scharpf M, Fend F, Noell S, Tatagiba M, and Brucker S, et al (2015). Residual gammaH2AX foci after ex vivo irradiation of patient samples with known tumour-type specific differences in radio-responsiveness. *Radiother Oncol* **116**, 480–485.

[58] Rath BH, Wahba A, Camphausen K, and Tofilon PJ (2015). Coculture with astrocytes reduces the radiosensitivity of glioblastoma stem-like cells and identifies additional targets for radiosensitization. *Cancer Med* **4**, 1705–1716.